SOLID-STATE COOLING

Highly efficient electrocaloric cooling with electrostatic actuation

Rujun Ma,[1]* Ziyang Zhang,[1]* Kwing Tong,[1] David Huber,[2] Roy Kornbluh,[2] Yongho Sungtaek Ju,[3] Qibing Pei[1]†

Solid-state refrigeration offers potential advantages over traditional cooling systems, but few devices offer high specific cooling power with a high coefficient of performance (COP) and the ability to be applied directly to surfaces. We developed a cooling device with a high intrinsic thermodynamic efficiency using a flexible electrocaloric (EC) polymer film and an electrostatic actuation mechanism. Reversible electrostatic forces reduce parasitic power consumption and allow efficient heat transfer through good thermal contacts with the heat source or heat sink. The EC device produced a specific cooling power of 2.8 watts per gram and a COP of 13. The new cooling device is more efficient and compact than existing surface-conformable solid-state cooling technologies, opening a path to using the technology for a variety of practical applications.

Vapor-compression refrigeration systems—commonly used in air conditioners for buildings and automobiles, refrigerators for food storage, and processing plants—rely on the phase change of refrigerants driven by mechanical compressors, a technology developed more than a century ago. Although effective for many applications, vapor-compression systems have their disadvantages. They are bulky, complex, and difficult to scale down to meet the cooling demands of modern technologies, such as mobile devices, wearable electronics, and flexible electronics. The coefficient of performance (COP), the amount of heat removed per electrical energy consumed, is also low, typically 2 to 4 for vapor-compression refrigerators (*1*, *2*).

Solid-state cooling systems are more recent alternatives that eliminate the need for compressors and conventional liquid or vapor refrigerants, whose growing usage, improper management, and disposal have considerable global warming potential (*3*). Thermoelectric coolers based on the Peltier effect produced in bismuth antimony telluride ceramic elements have been found to have a number of applications. However, these systems typically exhibit a COP lower than that of vapor-compression refrigeration systems (*4*). Further, the ceramic materials tend to be expensive, restricting their feasibility to small-scale applications where the amount of material is small or cost is not a dominant factor (*5*). Solid-state refrigeration based on the electrocaloric (EC) effect has been proposed as a more efficient alternative that can also be used to realize compact low-profile devices (*2*, *6*–*8*). The EC effect is a thermodynamic phenomenon where a reversible temperature change of a dielectric material is achieved through the modulation of its dipolar entropy under an applied electric field (see fig. S1) (*7*).

Current EC materials such as relaxor ferroelectric ceramics (*6*) and polymers (*7*) have promising material properties. Lead zirconium titanate ($PbZr_{0.95}Ti_{0.05}O_3$) exhibits a large adiabatic temperature change (ΔT) of 12°C at 226°C. Various poly(vinylidene fluoride) (PVDF)–based ferroelectric polymers are interesting because of their large isothermal entropy change, light weight, and adaptability to complex form factors and low-temperature processing conditions. Among this class of polymers, poly(vinylidene fluoride-*ter*-trifluoroethylene-*ter*-chlorofluoroethylene) [P(VDF-TrFE-CFE)] has a calculated ΔT of 12°C at 55°C (*7*). Nanocomposites composed of either P(VDF-TrFE-CFE) or P(VDF-TrFE) with nanosized boron nitride or other ceramics have similarly high EC performance (*8*).

Even though numerous publications have reported high material-level performances, the realization of practical solid-state cooling devices based on the EC effect remains a major challenge. Previously reported EC cooling devices (*9*–*15*) have no experimentally obtained COP data. The highest reported specific cooling power of 0.018 W/g (*15*) is orders of magnitude smaller than the theoretically calculated values based on intrinsic material properties. One critical challenge of implementing EC cooling devices stems from the fact that the EC polymer material must cyclically make and break thermal contact between the heat source and heat sink. Thus, an actuator such as an electric motor may be used. Such actuators lower the COP and increase the size and complexity of the system. Alternative EC designs use pumps to move fluid that carries the heat between the heat source, heat sink, and EC polymer stack (*15*, *16*). However, this approach also increases the complexity and adds mass as well as additional energy losses from the pumping of the fluid.

We report an EC refrigeration–device architecture (Fig. 1) where we use electrostatic actuation to rapidly transport a flexible EC polymer stack between a heat source and a heat sink. The electrostatic force not only moves the EC material but also promotes the formation of intimate thermal contact between the EC polymer stack and the heat source and heat sink during each cycle. We developed a compact solid-state cooling device (7 cm by 3 cm by 0.6 cm) with a COP of 13 at a heat flux of 29.7 mW/cm^2 and a specific cooling power of 2.8 W/g, which is higher than other magnetocaloric, elastocaloric (*17*–*26*), and thermoelectric devices (see table S1). For example, the present EC device has a much better performance than the large-scale magnetocaloric refrigerator, which has a COP of 1.9 and a specific cooling power of 2 W/g (*17*). Further, the thin-film EC cooling device is flexible and can conform to surfaces with complex curvature. The device also operates without the noise and complexity of a conventional cooling system.

We selected P(VDF-TrFE-CFE) as the active EC material because of its large entropy change, large ΔT near room temperature, and mechanical flexibility (*7*). We used single-walled carbon nanotubes (CNTs) to form the electrodes of the EC film because of their mechanical compliance, thermal stability, and oxidation resistance (*27*, *28*). We drop-cast the P(VDF-TrFE-CFE) solution onto a glass substrate, and the resulting polymer film was heated at 90°C. We spray-coated a dispersion of CNTs in an isopropyl alcohol and water mixture onto the polymer film. We laminated one of the as-prepared films directly to the top of another, with one CNT layer sandwiched between the EC films. The overlap of the CNT areas (areas with electrodes on both sides of the film) defined the active area (2 cm by 5 cm) for the EC effect. We also spray-coated the bottom surface of the stack with CNTs to complete the fabrication of a two-layer EC polymer stack (Fig. 1). We then placed the EC laminate in a vacuum oven at 120°C for 16 hours to remove the residual solvent, raise the degree of crystallinity (see fig. S2), and enhance the polarizability of the polymer (*29*). The total mass of the EC laminate was 0.23 g.

The EC cooling device comprises two laminated sheets that are 7 cm by 3 cm in area and separated by a 6-mm-thick spacer made of poly(methyl methacrylate). Each laminate sheet consists of a double-sided Kapton tape, a polyimide film, and a silver-nanowire percolation network layer inserted in between. The nanowire percolation layer acts as one electrode of the electrostatic actuator. We mounted the EC polymer stack on one end of the EC device between the left spacer and the lower laminate sheet, and the other end between the right spacer and the upper laminate sheet (Fig. 1, A and B). For testing convenience, we attached a 6.3-mm-thick aluminum plate to the outer sticky surface of each of the Kapton tape layers. The bottom and top plates act as the heat source and heat sink, respectively. We inserted a heat flux sensor composed of a thermopile of thermocouples across a polyimide sheet [OMEGA heat flux sensor HFS-4, 2.06 μV/(W/m^2)] between

[1]Department of Materials Science and Engineering, Henry Samueli School of Engineering and Applied Science, University of California, Los Angeles, CA 90095, USA. [2]SRI International, 333 Ravenswood Avenue, Menlo Park, CA 94025, USA. [3]Department of Mechanical and Aerospace Engineering, University of California, Los Angeles, CA 90095, USA.
*These authors contributed equally to this work. †Corresponding author. Email: qpei@seas.ucla.edu

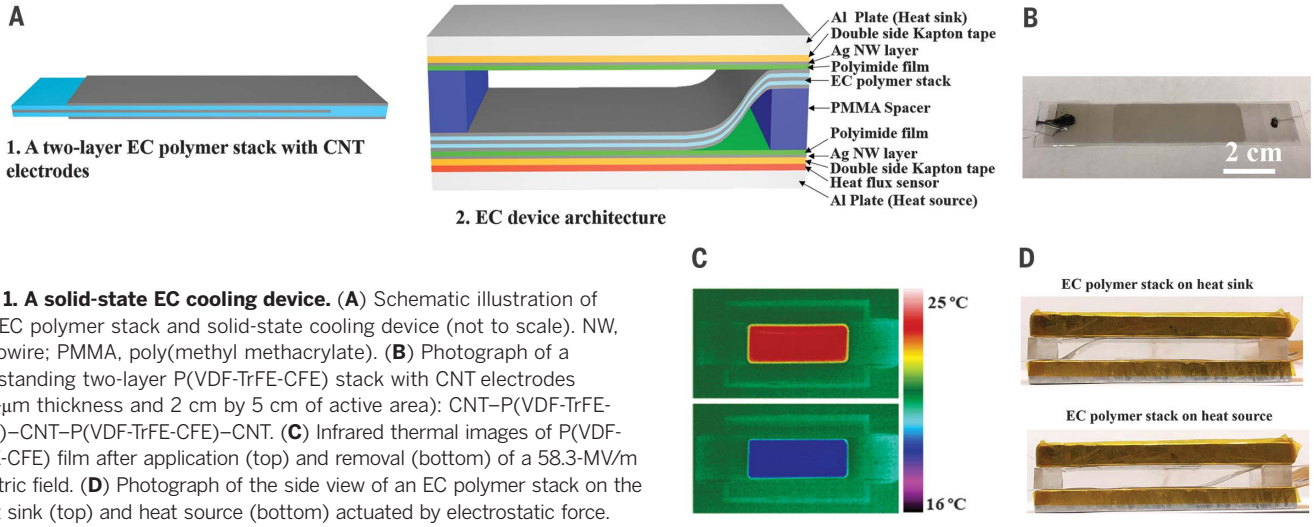

Fig. 1. A solid-state EC cooling device. (**A**) Schematic illustration of the EC polymer stack and solid-state cooling device (not to scale). NW, nanowire; PMMA, poly(methyl methacrylate). (**B**) Photograph of a freestanding two-layer P(VDF-TrFE-CFE) stack with CNT electrodes (60-μm thickness and 2 cm by 5 cm of active area): CNT–P(VDF-TrFE-CFE)–CNT–P(VDF-TrFE-CFE)–CNT. (**C**) Infrared thermal images of P(VDF-TrFE-CFE) film after application (top) and removal (bottom) of a 58.3-MV/m electric field. (**D**) Photograph of the side view of an EC polymer stack on the heat sink (top) and heat source (bottom) actuated by electrostatic force.

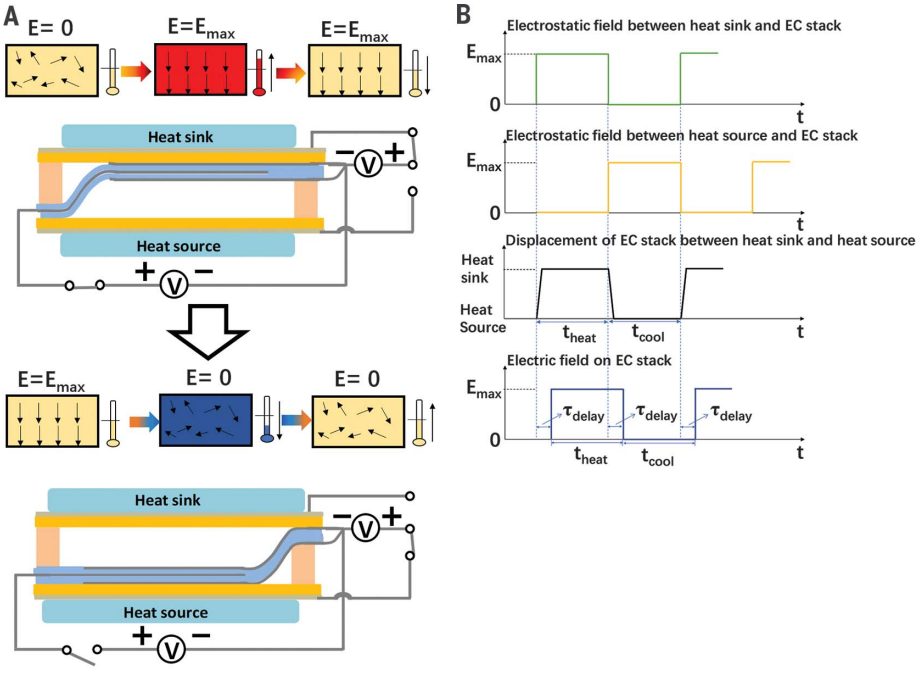

Fig. 2. Working mechanism of P(VDF-TrFE-CFE) cooling device to move heat from heat source to heat sink by electrostatic actuation. (**A**) Schematic showing how the electrostatic field drives the actuation of the EC polymer stack toward the heat sink or heat source and the respective position of the EC polymer film during operation of the device. By correlating the electric field of the EC polymer stack with the electrocaloric cycle, heat transfer from the heat source to the heat sink can be achieved. (**B**) Time domain illustration of the cooling cycle.

the aluminum plate heat source and the Kapton tape for in situ thermal measurement. A cross-sectional view of the EC polymer stack shows that it forms an S shape. The stationary ends of the S-shaped film allow the film to make good thermal contact with the electrodes of the top or bottom aluminum plate (*30*). During operation, the S-shaped EC film moves up and down like a flexure spring, driven by electrostatic forces when a voltage is applied between one of the silver-nanowire layers and the corresponding outer CNT layer on the EC stack that faces the silver-nanowire layer. Because of its light weight and low bending stiffness, the EC stack could be shuttled rapidly between attachment to the upper and lower laminates with a response time of less than 30 ms and total energy consumption of only ~0.02 W. This electrostatic actuation is compact, noiseless, and does not incur substantial frictional forces that could induce material damage and cause energy consumption, and thus parasitic heating. The instantaneous (adiabatic) temperature increase of the EC stack (Fig. 1C) when an electric field is applied results from the dipole orientation in the relaxor ferroelectric polymer and consequent decrease of entropy in the system (fig. S3).

The actuation of the polymer stack is achieved by applying an electrostatic field across the polyimide film of either the bottom or top plate to drive the movement of the EC polymer stack (Fig. 1D). The electric field across the air gap determines the electrostatic force that acts to move the EC polymer stack. The electrostatic forces also determine the pressure between the EC film and the heat source and heat sink. The pressure between the film and the top and bottom sheets that contact the heat source and heat sink, assuming that the thickness ($d_{polyimide}$) of the polyimide layer is much greater than its surface roughness, is (*31*)

$$P_{contact} = \varepsilon_0 \varepsilon_{r,polyimide} E_{contact}^2 = \frac{\varepsilon_0 \varepsilon_{r,polyimide} V^2}{d_{polyimide}^2} \quad (1A)$$

where E is the applied electrostatic field, ε_0 is vacuum permittivity, and $\varepsilon_{r,polyimide}$ = 4 is the dielectric constant of polyimide. Under an applied electrostatic field of 61 MV/m, this pressure is about 133 kPa (1.32 atm) (fig. S4). Away from the attachment point, the pressure is dominated by the air gap. The air gap is largest at the point where the film attaches to the opposite electrode. The pressure at this point is

$$P_{gap} = \varepsilon_0 \varepsilon_{r,air} E_{gap}^2 = \frac{\varepsilon_0 \varepsilon_{r,air} V^2}{d_{gap}^2} \quad (1B)$$

Because d_{gap} >> $d_{polyimide}$ and $\varepsilon_{r,air}$ = 1, this pressure is much lower. Although P_{gap} away from the contact point may not be great enough to move the EC stack, the bending of the film allows for the film to progressively attach a greater length of its surface to the active electrode (that to which the voltage is applied). That is, the attachment point moves across the length of the film until all of the film, except for the small section needed

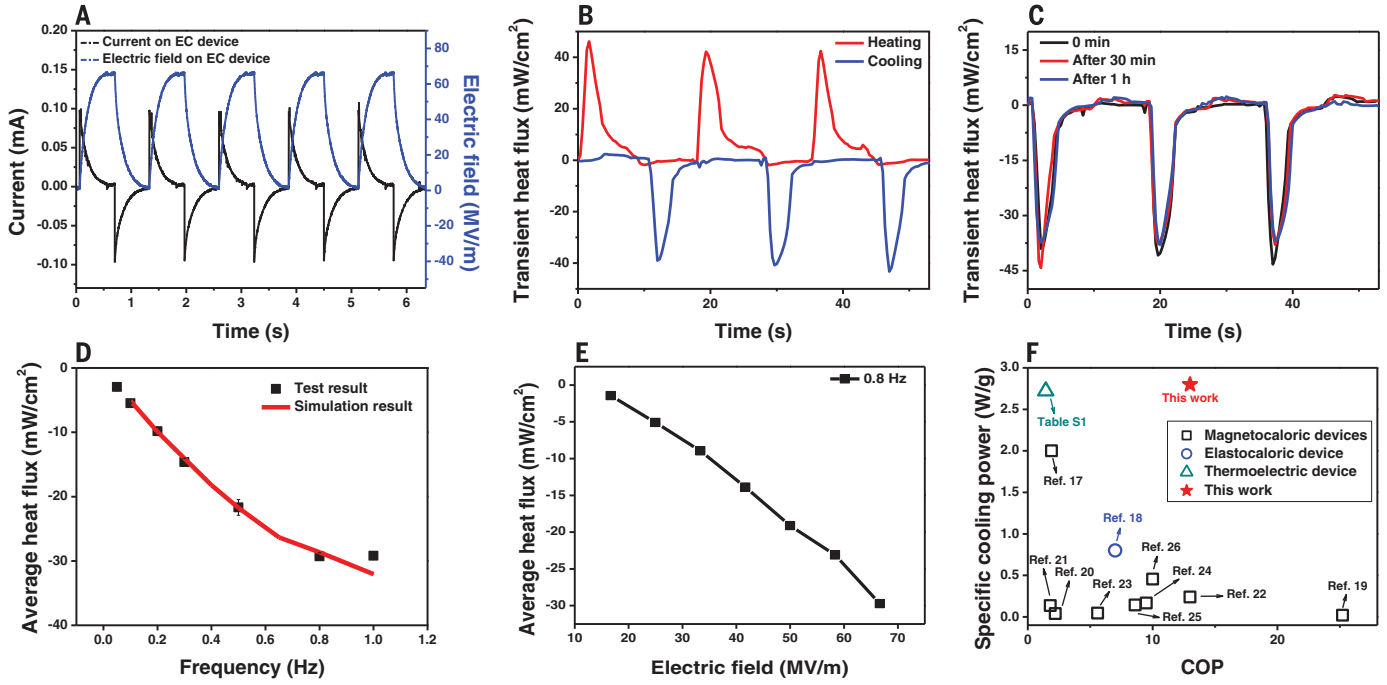

Fig. 3. Performance of the EC polymer cooling device. (**A**) Power consumption of EC film under an applied electric field of 66.7 MV/m. (**B**) Comparison of heat flux measured by the heat flux sensor in both heating and cooling modes with an applied electric field of 50 MV/m and frequency of 0.06 Hz. (**C**) Cyclic testing of heat movement transport from the heat source to the EC polymer stack with an applied electric field of 50 MV/m and frequency of 0.06 Hz. (**D**) Heat flux as a function of different frequencies of operation. Simulation results, which were obtained by numerically solving the transient heat conduction equation with the finite volume method, agree well with the experimental value. (**E**) Heat flux of EC polymer film as a function of different applied electric fields at 0.8 Hz. (**F**) Specific cooling power with corresponding COP is compared with those of magnetocaloric, elastocaloric, and thermoelectric devices reported in the literature.

to span the attachment point to the opposite electrode, has moved to the active electrode. This approach to electrostatic actuation may be used when the bending stiffness of the film can be overcome by the electrostatic forces. The shape of the edge of the film gives this type of actuator the name "S-shaped film actuator" (*30*). Such electrostatic actuation has been used to move films for valving.

When an electric field is alternately applied across the top silver-nanowire electrode and the top CNT layer of the EC stack and the bottom silver-nanowire electrode and the bottom CNT layer of the EC stack, the EC polymer stack shuttles between the two aluminum plates. The electrostatic pressure on the film (Eq. 1A) increases the thermal contact between the EC-stack film and polyimide and thus facilitates the heat flux between the EC material and the aluminum plates. This high thermal contact is confirmed by the measured heat flux during the cooling cycle of an EC polymer stack when an electric field of 66.7 MV/m (square wave, 0.8 Hz) was applied across the P(VDF-TrFE-CFE) films.

The operating cycle consists of six steps: (i) electrostatic actuation of the EC polymer stack toward the top aluminum plate (heat sink); (ii) electrocaloric heating of the EC polymer stack; (iii) heat transfer from the EC polymer stack to the heat sink; (iv) electrostatic actuation of the EC polymer stack toward the bottom aluminum plate (heat source); (v) electrocaloric cooling of the EC polymer stack; and (vi) heat transfer from the heat source to the EC polymer stack (Fig. 2). For simplicity of circuitry design, we fabricated the EC cooling device with a common cathode by connecting the two outer CNT electrodes of the EC polymer stack with a thin copper wire. The inner (middle) CNT electrode of the EC polymer stack serves as the anode to apply an electric field across the P(VDF-TrFE-CFE) film for electrocaloric heating. The silver-nanowire films function as the anode to apply an electrostatic field across the polyimide for electrostatic actuation. We controlled the voltage switching for electrostatic actuation by an electric relay to switch between the silver-nanowire anodes of the heat source and

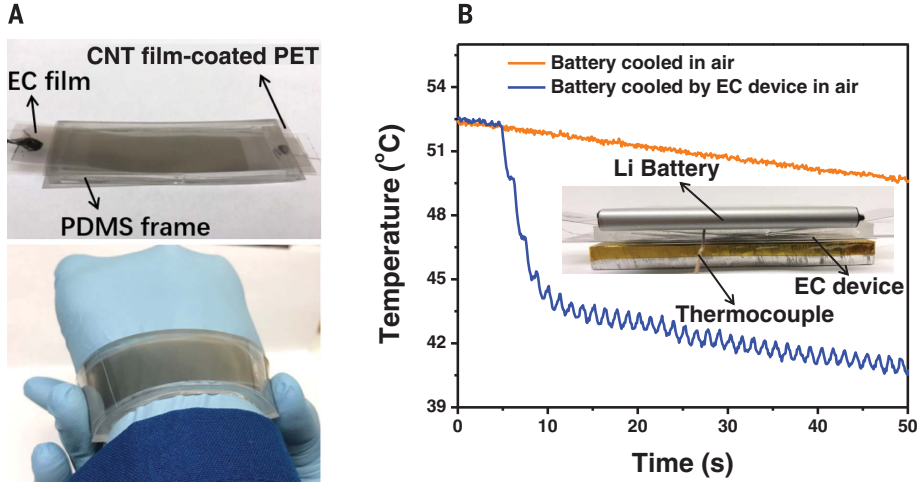

Fig. 4. Performance of the flexible EC cooling device. (**A**) Photograph of a flexible EC device. PDMS, poly(dimethylsiloxane). (**B**) Temperature change of an overheated smartphone battery with and without an EC cooling device. The inset shows an overheated battery on the top of the EC device.

heat sink. During one cycle of heat transfer, an electrostatic field is first applied between the silver nanowire on the heat sink and the outer CNT electrodes to generate an electrostatic pressure to transport the EC polymer stack toward the heat sink. The time required to move the EC polymer stack from the heat source to the heat sink is roughly 0.03 s, but a short delay (τ_{delay} = 0.15 s) is preprogrammed in the EC waveform to allow for the EC polymer stack to form sufficient thermal contact with the polyimide before applying an electric field across the P(VDF-TrFE-CFE) film. When an electric field is applied across the P(VDF-TrFE-CFE) film for electrocaloric heating, and the molecular dipoles become aligned, the resulting decrease in entropy increases the temperature of the EC polymer film (for further information, see the supplementary materials). A temperature gradient is thus created, causing heat to be transferred from the EC polymer stack to the heat sink. After a predefined time of heating, t_{heat}, the electrostatic actuation is switched by using the electric relay to transport the EC polymer film toward the heat source. After another short delay, τ_{delay}, electrocaloric cooling occurs by switching off the electric field across the P(VDF-TrFE-CFE) film to allow for the dipoles within the polymer to become randomly aligned. The entropy of the film increases while heat is transferred from the heat source to the EC polymer stack during a predefined time of cooling, t_{cool}, thus completing one cycle of heat transfer.

We investigated the power consumption of the P(VDF-TrFE-CFE) cooling device. The electric energy consumption of the EC device can be calculated with

$$W_{EC} = \int_{t1}^{t2} V_{EC} \times I_{EC} dt \qquad (2)$$

where W_{EC} is the electrical work done in one EC cycle and V_{EC} and I_{EC} are the measured operating voltage and current, respectively (see fig. S5). The start and end times of an entire EC cycle are t1 and t2, respectively. The power consumption averaged over one cycle is 2 mW/cm^2 under an applied electric field of 66.7 MV/m and an electrostatic field of 61 MV/m at 0.8 Hz (Fig. 3A). We found insignificant leakage when compared to the charging and discharging currents of the EC film. We observed no heat flux when the P(VDF-TrFE-CFE) cooling device operated without an electric field, indicating negligible joule heating, from the electrostatic actuation or losses associated with the motion of the film. We also found insignificant joule heating from the EC effect (Fig. 3B). Verifying that the measured effects are not transient, we found that the heat flux of the P(VDF-TrFE-CFE) cooling device after continuous operation for >1 hour was the same as the initial heat flux (Fig. 3C).

We increased the average heat flux of the cooling device by operating at a higher frequency (Fig. 3D). Although the electrostatic actuation of the EC polymer stack can operate at higher frequencies, the frequency of the P(VDF-TrFE-CFE) cooling device that gives maximum heat flux is 0.8 Hz, due in part to the time needed to transfer the heat from the EC material to the laminate sheets at the heat source and heat sink. Another way to maximize heat flux is by increasing the electric field of the EC polymer stack. Figure 3E shows the heat flux of a P(VDF-TrFE-CFE) cooling device operated at a frequency of 0.8 Hz as a function of the applied electric field. At a frequency of 0.8 Hz, the maximum electric field was set at 66.7 MV/m to avoid electrical instability of the P(VDF-TrFE-CFE) cooling device. Further refinement of the material processing or lamination techniques could allow for an increase in the maximum electric field and thus allow for substantially greater heat flow per cycle. The EC polymer stack did not show any sign of electrical failure or other damage after 30,000 cycles of charging-discharging (fig. S6). We achieved a heat flux of 29.7 mW/cm^2 with an applied electric field across the EC film of 66.7 MV/m, and this corresponds to a specific cooling power of 2.8 W/g. This specific cooling power is 150 times the reported cooling power of 0.018 W/g, calculated on the basis of experimentally obtained heat flux data of ceramic EC devices (*15*).

We also calculated the $\mathrm{COP} = \frac{Q_{transferred}}{W_{in}} = \frac{\text{heat transferred}}{\text{electrical work in}} = 13$. The temperature differential between the aluminum heat sink and heat source was 1.4 K.

It is easier to obtain a larger COP if the temperature difference between the heat source and heat sink is small. The COP relative to the ideal (Carnot) COP is often used to account for comparisons between different temperature spans. Figure S8 shows the COP and $\mathrm{COP/COP_{Carnot}}$, as well as the heat flux, as a function of the temperature span. We conducted an analysis to compare our technology on this basis (see table S1). Our $\mathrm{COP/COP_{Carnot}}$ is 0.061 at the ΔT of 1.4 K. This value is below that of the best values reported for magnetocaloric and elastocaloric materials. However, our specific power is greater. Although thermoelectric devices can, in principle, have a greater $\mathrm{COP/COP_{Carnot}}$ at low temperature spans, the $\mathrm{COP/COP_{Carnot}}$ at similar specific heat flux values (as shown in table S1) is typically much lower.

We identified approaches that can further improve the performance of our device. When the aluminum heat sink and heat source were replaced by carbon nanotube–coated polyethylene terephthalate (PET) films (thickness of 100 μm), the temperature span was increased to 2.8 K (fig. S7). In addition, it is worthwhile to note that, given the dielectric nature of EC polymer, energy recovery is possible during the depolarization process, which would further enhance the efficiency. The specific cooling power and COP puts this device in a different operational space when compared to elastocaloric (*18*), magnetocaloric (*17*, *19*–*26*), and thermoelectric (see table S1) devices reported in the literature (Fig. 3F).

We demonstrated the benefits of the inherent thinness and flexibility of our cooling device by fabricating a version that can conform to a nonflat surface—a smartphone battery (Samsung Galaxy S4). The P(VDF-TrFE-CFE) cooling device consisted of a transparent flexible frame made of conductive CNTs coated on a 100-μm-thick PET film that serves as the laminate sheet for electrostatic actuation (Fig. 4A). We fixed the S-shaped EC polymer stack to a polydimethylsiloxane 4-mm-thick frame spacer. The device size is 7 cm by 3 cm by 0.5 cm. Under high workloads in a smartphone, the battery heats up to 52.5°C. When allowed to cool in air, the surface temperature of the battery, measured with a surface-mount thermocouple, decreased by 3°C in 50 s (Fig. 4B). After the flexible EC cooling device was attached to the battery, the surface temperature of the battery was observed to decrease by 8°C in the first 5 s with EC cooling activated under an applied field of 66.7 MV/m at 0.8 Hz. Overheating of smartphone batteries under high workloads creates a fire hazard, and prolonged use under thermal overload causes reduced battery lifetime and fatigue of other materials and components in the smartphone. Our flexible cooling approach could help mitigate this problem. The high COP, high heat flux, compact- and flexible-form factor should find application in wearable and mobile devices where no current active-cooling technologies are suitable.

REFERENCES AND NOTES

1. X. Li, thesis, The Pennsylvania State University (2013).
2. T. Correia, Q. Zhang, Eds., *Electrocaloric Materials: New Generation of Coolers* (Springer, 2014).
3. P. Hawken, Ed., *Drawdown: The Most Comprehensive Plan Ever Proposed to Reverse Global Warming* (Penguin Books, 2017).
4. J. W. Peeples, *Electronics Cooling Magazine* **7**, 16–24 (2001).
5. I. Chowdhury *et al*., *Nat. Nanotechnol.* **4**, 235–238 (2009).
6. A. S. Mischenko, Q. Zhang, J. F. Scott, R. W. Whatmore, N. D. Mathur, *Science* **311**, 1270–1271 (2006).
7. B. Neese *et al*., *Science* **321**, 821–823 (2008).
8. Q. Li *et al*., *Adv. Mater.* **27**, 2236–2241 (2015).
9. Y. Jia, Y. Sungtaek Ju, *Appl. Phys. Lett.* **100**, 242901 (2012).
10. R. I. Epstein, K. J. Malloy, *J. Appl. Phys.* **106**, 064509 (2009).
11. Y. S. Ju, *J. Electron. Packag.* **132**, 041004 (2010).
12. Y. V. Sinyavsky, V. M. Brodyansky, *Ferroelectrics* **131**, 321–325 (1992).
13. H. M. Gu *et al*., *Appl. Phys. Lett.* **102**, 122904 (2013).
14. U. Plaznik *et al*., *Appl. Phys. Lett.* **106**, 043903 (2015).
15. Y. D. Wang *et al*., *Appl. Phys. Lett.* **107**, 134103 (2015).
16. M. Ožbolt, A. Kitanovski, J. Tušek, A. Poredoš, *Int. J. Refrig.* **40**, 174–188 (2014).
17. S. Jacobs *et al*., *Int. J. Refrig.* **37**, 84–91 (2014).
18. J. Tušek *et al*., *Nature Energy* **1**, 16134 (2016).
19. Q. Gao *et al*., *Int. J. Refrig.* **29**, 1274–1285 (2006).
20. P. Clot *et al*., *IEEE Trans. Magn.* **39**, 3349–3351 (2003).
21. T. Okamura, R. Rachi, N. Hirano, S. Nagaya, in *Proceedings of the 2nd International Conference on Magnetic Refrigeration at Room Temperature* (Portoroz, Slovenia, 2007), pp. 281–288.
22. C. Zimm, J. Auringer, A. Boeder, J. Chell, S. Russek, A. Sternberg, in *Proceedings of the 2nd International Conference on Magnetic Refrigeration at Room Temperature* (Portoroz, Slovenia, 2007), pp. 341–347.
23. N. Hirano *et al*., *AIP Conf. Proc.* **613**, 1027–1034 (2002).
24. C. Zimm *et al*., *Adv. Cryog. Eng.* **43**, 1759–1766 (1998).
25. J. A. Lozano *et al*., *Appl. Energy* **111**, 669–680 (2013).
26. A. Tura, A. Rowe, *Int. J. Refrig.* **34**, 628–639 (2011).
27. R. Ma *et al*., *Adv. Mater.* **24**, 3344–3349 (2012).
28. W. Yuan *et al*., *Adv. Mater.* **20**, 621–625 (2008).
29. L. Engel, S. Kruk, J. Shklovsky, Y. Shacham-Diamand, S. Krylov, *J. Micromech. Microeng.* **24**, 125027 (2014).
30. K. Sato, M. Shikida, *J. Micromech. Microeng.* **4**, 205–209 (1994).
31. R. Pelrine, R. Kornbluh, Q. Pei, J. Joseph, *Science* **287**, 836–839 (2000).

ACKNOWLEDGMENTS
This work was supported by the Advanced Research Projects Agency–Energy (award no. DE-AR0000532) and the Air Force Office of Scientific Research (grant no. FA9550-15-1-0340). All results are reported in the main text and supplementary materials. Q.P., R.M., Z.Z., R.K., and D.H. are inventors on U.S. provisional patent application serial number 62/502,251, submitted jointly by University of California–Los Angeles and SRI, that covers the structure and preparation of the electrocaloric devices. R.M., Z.Z., D.H., R.K., and Q.P. conceived and designed the experiments; R.M. prepared EC polymer stacks; R.M. and Z.Z. fabricated the devices; R.M., Z.Z., D.H., and R.K. performed the measurements; R.M., Z.Z., K.T., D.H., R.K., Y.S.J., and Q.P. analyzed and interpreted the data; R.M., Z.Z., and Y.S.J. simulated the device performance; R.M., Z.Z., K.T., D.H., R.K., and Q.P. organized the data and wrote the manuscript; R.M., R.K., Y.S.J., and Q.P. revised the manuscript; and all authors reviewed and commented on the manuscript.

SUPPLEMENTARY MATERIALS
www.sciencemag.org/content/357/6356/1130/suppl/DC1
Materials and Methods
Figs. S1 to S8
Table S1
References (*32*–*34*)

5 May 2017; accepted 17 July 2017
10.1126/science.aan5980

Science

Highly efficient electrocaloric cooling with electrostatic actuation

Rujun Ma, Ziyang Zhang, Kwing Tong, David Huber, Roy Kornbluh, Yongho Sungtaek Ju and Qibing Pei

Science **357** (6356), 1130-1134.
DOI: 10.1126/science.aan5980

A solid way to keep cool

Refrigeration relies on vapor compression that is noisy, takes up space, and is mechanically complex. Solid-state cooling requires changing an external field to drive cooling, but devices produced so far have not been efficient enough for practical applications. Ma *et al.* constructed a lightweight and flexible device using a thin electrocaloric polymer film, where toggling it in an electric field between a heat source and sink drives the cooling process (see the Perspective by Zhang and Zhang). The device rapidly cools down an overheated smartphone battery and has potential application for developing compact, low-profile electronics.

Science, this issue p. 1130; see also p. 1094

Science (print ISSN 0036-8075; online ISSN 1095-9203) is published by the American Association for the Advancement of Science, 1200 New York Avenue NW, Washington, DC 20005. The title *Science* is a registered trademark of AAAS.